Polyhedron 117 (2016) 826–833

Contents lists available at ScienceDirect

Polyhedron

journal homepage: www.elsevier.com/locate/poly

Synthesis, structure, and chromogenic properties of polymethylene-vaulted *trans*-bis(salicylaldiminato)palladium(II) complexes

Takatoshi Maeda, Soichiro Kawamorita, Takeshi Naota *

Department of Chemistry, Graduate School of Engineering Science, Osaka University, Machikaneyama, Toyonaka, Osaka 560-8531, Japan

ARTICLE INFO

Article history:
Received 11 March 2016
Accepted 2 May 2016
Available online 9 May 2016

Keywords:
Photophysics
Palladium(II)
Schiff bases
X-ray diffraction
Density function theory

ABSTRACT

The synthesis, structure, and chromogenic properties of polymethylene-vaulted *trans*-bis(salicylaldiminato)palladium(II) complexes are described. A series of the Pd complexes incorporating nona-, deca-, undeca- and dodecamethylene bridges (**1a**: $n = 9$; **1b**: $n = 10$; **1c**: $n = 11$; **1d**: $n = 12$) was prepared by the treatment of $Pd(OAc)_2$ with the corresponding *N*,*N*′-bis(salicylidene)-1,ω-alkanediamines. The *trans*-coordination, vaulted structures, and crystal packing of **1a**–**d** have been unequivocally established from X-ray diffraction studies. Complexes **1a**–**d** exhibit linker-dependent chromatic properties in 2-methyl-2,3,4,5-tetrahydrofuran, where the absorption wavelengths at around 400 nm are shifted hypsochromically with a decrease in the linker length, which is in contrast to the structure-independence of the absorption properties for the corresponding polymethylene-vaulted Pt analogues **2a**–**d** observed under the same conditions. Density functional theory and time-dependent DFT calculations revealed that the present specific linker dependence in the chromism of **1** is ascribed to specific alteration of the d–π conjugation on the flexible *trans*-bis(salicylaldiminato)palladium coordination platforms by variation of the coordination planarity.

1. Introduction

Vaulted transition metal complexes with bridging structures over coordination platforms have attracted much interest as new candidates for functional materials because they are expected to provide potential controllability of the three-dimensional (3D) conditions around the metals upon bridging based molecular alteration [1–3]. A variety of vaulted complexes with bridging ligands including porphyrins [2,4], macrocyclic tetraimines [5], *o*-iminophenols [6–8], *N*-heterocyclic carbenes [9], *o*-(aminomethyl)phenols [10], *o*-iminoketones [11], *o*-iminopyrroles [12], bipyridines [13], 2-aminotropones [14], and diphosphines [1,3,15,16], have been synthesized and investigated with respect to their photophysical [4d,6b,8,9b], association [4a,5,7a] and aggregation [6a,6b,14] properties, molecular mobility [1,7,15], and catalytic activity for organic transformations [2,3,4b,4c,9a,16].

As part of our program towards the formation of functional transition metal-based materials with 3D superstructures, we have been investigating the development of new functions of flexible *trans*-bis(salicylaldiminato) coordination platforms of d^8 transition metals based on molecular alteration with flexible polymethylene bridges [6–8]. Vaulted, clothespin-shaped binuclear complexes of Pd(II) and Pt(II) metals exhibit stimuli–responsive aggregation properties upon brief irradiation with ultrasonic waves [6]. Polymethylene and poly(ethyleneglycol)-vaulted Pt(II) complexes in the crystalline state exhibit intense phosphorescent emission under UV excitation at ambient temperature [8]. These unprecedented phenomena can be remotely controlled by the type and length of the bridged linker, mainly based on the subsequent alteration of the d–π conjugation and the special 3D structure around the coordination platforms. Here, we have focused on the correlation between the molecular structure and chromogenic properties of polymethylene-vaulted mononuclear Pd analogues. For this purpose, a series of novel *trans*-bis(salicylaldiminato)Pd(II) complexes (**1**), incorporating nona- (**a**), deca- (**b**), undeca- (**c**) and dodecamethylene (**d**) bridges, were synthesized and compared with the corresponding Pt analogues **2** [8a,b,g] in terms of the molecular structure, photophysical properties and electronic configurations. The specific linker-dependent change in chromogenic properties of **1**, and the contrasting independence of the Pt analogues **2** was discussed based on the density functional theory (DFT) and time-dependent DFT (TD-DFT) calculations focusing on the change in d–π conjugation of the flexible coordination platform by molecular alteration with variation of the linker length. Here, we describe the synthesis, structure and chromogenic properties of

* Corresponding author. Fax: +81 6 6850 6222.
E-mail address: naota@chem.es.osaka-u.ac.jp (T. Naota).

http://dx.doi.org/10.1016/j.poly.2016.05.004
0277-5387/

complexes **1** bearing a line of short and long polymethylene linkers, with special attention given to comparison with the contrasting properties of the Pt analogues.

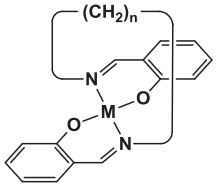

1: M = Pd **a**: n = 9
2: M = Pt **b**: n = 10
c: n = 11
d: n = 12

2. Experimental

2.1. Spectroscopic methods

IR spectra were measured using a Shimadzu IR Prestige-21 spectrometer. ^{1}H and ^{13}C NMR spectra were recorded with a Varian Unity-Inova 500 spectrometer. Mass spectra were obtained with a Jeol JMS-DX 303 spectrometer. UV/Vis spectra of solutions were measured using a Jasco V-650 spectrometer. Elemental analyses were performed with a Perkin–Elmer 2400II CHN elemental analyzer.

2.2. Preparation of palladium complexes ***1a–d***

A mixture of $Pd(OAc)_2$ (0.449 g, 2.00 mmol), the corresponding *N*,*N*′-bis(salicylidene)-1,ω-alkanediamine (2.00 mmol), and triethylamine (0.810 g, 8.00 mmol) in toluene (300 mL) was refluxed for 5 h. After evaporation of the solvent under reduced pressure, the residue was poured into a mixture of EtOAc (200 mL) and water (100 mL). The resulting organic layer was washed with water, dried over $MgSO_4$, and concentrated under reduced pressure to give the crude product as an orange solid. Column chromatography (SiO_2, toluene) afforded **1a–d** as orange solids. The complexes **1** were recrystallized from EtOH for photophysical and single crystal X-ray diffraction (XRD) studies, and their purities for photophysical measurements were confirmed by NMR, elemental and high-performance liquid chromatography (HPLC) analyses. Melting points were measured in a glass capillary using a Büchi B-545 melting point apparatus.

2.2.1. Complex ***1a***

Orange block (38%). M.p. 188–191 °C; IR (KBr, cm^{-1}) 3021, 2920, 2858, 1623, 1597, 1538, 1443, 1305, 1146, 751; ^{1}H NMR ($CDCl_3$, 500 MHz) δ: 1.51–1.60 (m, 6 H), 1.75–1.90 (m, 6H), 2.00–2.09 (m, 2 H), 2.16–2.25 (m, 2H), 3.05 (ddd, J = 12.0, 5.7, 5.7 Hz, 2H), 4.69 (ddd, J = 12.0, 9.3, 4.1 Hz, 2H), 6.86 (d, J = 8.6 Hz, 2H), 7.14 (dd, J = 7.8, 1.9 Hz, 2H), 7.19 (ddd, J = 8.6, 6.9, 1.9 Hz, 2H), 7.48 (s, 2H); ^{13}C NMR ($CDCl_3$, 125 MHz) δ: 25.2, 27.5, 28.5, 31.4, 56.0, 114.9, 120.7, 122.1, 133.6, 134.3, 161.4, 165.6; HRMS (FAB): *m*/*z* Calc. for $C_{23}H_{28}N_2O_2{}^{196}Pd$: 470.1186; found: 470.1188 [M$^+$].

2.2.2. Complex ***1b***

Orange block (25%). M.p. 181–185 °C; IR (KBr, cm^{-1}) 3022, 2929, 2855, 1623, 1597, 1536, 1442, 1348, 1319, 1148, 910, 753; ^{1}H NMR ($CDCl_3$, 500 MHz) δ: 1.30–1.60 (m, 10H), 1.64–1.74 (m, 2H), 1.74–1.84 (m, 2H), 2.44–2.54 (m, 2H), 2.86 (ddd, J = 12.0, 11.5, 4.0 Hz, 2H), 4.73 (ddd, J = 12.0, 4.6, 4.0 Hz, 2H), 6.54 (ddd, J = 7.8, 6.8, 1.8 Hz, 2H), 6.85 (d, J = 8.5 Hz, 2H), 7.14 (dd, J = 7.8, 1.8 Hz, 2H), 7.52 (s, 2H), 7.21 (ddd, J = 8.5, 6.8, 1.8 Hz, 2H); ^{13}C NMR ($CDCl_3$, 125 MHz) δ: 24.1, 26.4, 27.9, 29.6, 58.7, 114.7, 120.6, 121.0, 133.8, 134.2, 161.1, 165.3; HRMS (FAB): *m*/*z* Calc. for $C_{24}H_{30}N_2O_2{}^{196}Pd$: 484.1342; found: 484.1343 [M$^+$].

2.2.3. Complex ***1c***

Orange block (38%). M.p. 173 °C; IR (KBr, cm^{-1}) 3053, 2929, 2856, 1625, 1597, 1539, 1444, 1307, 1148, 759; ^{1}H NMR ($CDCl_3$, 500 MHz) δ: 1.31–1.43 (m, 4H), 1.45–1.58 (m, 10H), 1.67–1.79 (m, 2H), 2.24–2.36 (m, 2H), 2.82 (ddd, J = 11.0, 10.5, 3.1 Hz, 2H), 4.79 (ddd, J = 11.0, 4.5, 4.1 Hz, 2H), 6.54 (ddd, J = 7.8, 6.8, 1.8 Hz, 2H), 6.85 (d, J = 7.8 Hz, 2H), 7.15 (dd, J = 7.8, 1.8 Hz, 2H), 7.21 (ddd, J = 8.5, 6.8, 1.8 Hz, 2H), 7.51 (s, 2H); ^{13}C NMR ($CDCl_3$, 125 MHz) δ: 24.7, 26.4, 27.7, 27.9, 31.0, 58.2, 114.7, 120.6, 121.0, 133.9, 134.3, 161.3, 165.4; HRMS (FAB): *m*/*z* Calc. for $C_{25}H_{32}N_2O_2{}^{196}Pd$: 498.1499; found: 498.1501 [M$^+$]. *Anal.* Calc. for $C_{25}H_{32}N_2O_2Pd$: C, 60.18; H, 6.46; N, 5.61. Found: C, 59.92; H, 6.16; N, 5.56%.

2.2.4. Complex ***1d***

Orange block (61%). M.p. 141–142 °C; IR (KBr, cm^{-1}) 3051, 2920, 2849, 1622, 1538, 1446, 1326, 1149, 902, 750; ^{1}H NMR ($CDCl_3$, 500 MHz) δ: 1.15–1.23 (m, 2H), 1.30–1.60 (m, 16H), 2.12–2.23 (m, 2H), 2.82 (ddd, J = 11.3, 10.7, 3.1 Hz, 2H), 4.75 (ddd, J = 11.3, 4.5, 4.1 Hz, 2H), 6.55 (ddd, J = 7.8, 6.9, 1.1 Hz, 2H), 6.86 (dd, J = 8.7, 1.1 Hz, 2H), 7.16 (dd, J = 7.8, 1.8 Hz, 2H), 7.54 (s, 2H), 7.22 (ddd, J = 8.7, 6.9, 1.8 Hz, 2H); ^{13}C NMR ($CDCl_3$, 125 MHz) δ: 24.5, 27.5, 27.7, 28.1, 30.7, 58.1, 114.6, 120.5, 120.6, 134.0, 134.2, 161.5, 165.2; HRMS (FAB): *m*/*z* Calc. for $C_{26}H_{34}N_2O_2{}^{196}Pd$: 512.1655; found: 512.1646 [M$^+$].

2.3. X-ray structure determination

Crystals of **1a–d** suitable for XRD studies were prepared by recrystallization from EtOH (for **1a**, **1c**, and **1d**) and $CHCl_3$–EtOH (for **1b**), and analyzed using a Rigaku Mercury 70 CCD diffractometer and a Rigaku Osmic VariMax diffractometer with graphite-monochromated Mo Kα radiation (λ = 0.71075 Å). The structures of (±)-**1a**, (±)-**1b**, (±)-**1c**, and (±)-**1d** were solved by direct methods and refined using the full-matrix least-squares method. In subsequent refinements, the function $\sum\omega(F_o^2 - F_c^2)^2$ was minimized, where F_o and F_c are the observed and calculated structure factor amplitudes, respectively. The positions of non-hydrogen atoms were determined from difference Fourier electron-density maps and refined anisotropically. All calculations were performed with the Crystal Structure crystallographic software package, and illustrations were drawn using ORTEP [17]. Details of the structure determinations are given in Fig. 1 and Table 1.

2.4. Computational methods

All calculations were conducted on the basis of DFT with the B3LYP exchange–correlation functional [18] using the GAUSSIAN 09W [19] program package. The basis set used was the effective core potential (LanL2DZ) for palladium atoms [20] and 6-31G* for the remaining atoms [21]. Molecular orbitals and their eigenvalues for complexes **1a–d** and **2a–d** [8a,b,g] were calculated using the molecular geometries obtained from the structure optimization. The singlet–singlet transition energies (E(S_n)) were estimated by TD-DFT calculation (B3LYP/6-31G*, LanL2DZ) [22]. The results are shown in Tables 2 and 3, and Fig. 4, as well as in Figs. S5–S8 of the Supplementary data.